Fundamental Research xxx (xxxx) xxx

Contents lists available at ScienceDirect

Fundamental Research

journal homepage: http://www.keaipublishing.com/en/journals/fundamental-research/

Review

Lensless camera: Unraveling the breakthroughs and prospects

Shuowen Li[a], Yunhui Gao[a], Jiachen Wu[a], Mingjie Wang[b], Zhangcheng Huang[c], Shumei Chen[b], Liangcai Cao[a,*]

[a] Department of Precision Instruments, Tsinghua University, Beijing 100084, China
[b] Key Laboratory of Micro-Nano Optoelectronic Information System of Ministry of Industry and Information Technology, Harbin Institute of Technology, Shenzhen 518055, China
[c] State Key Laboratory of ASIC and System, Frontier Institute of Chip and System, Fudan University, Shanghai 200438, China

ARTICLE INFO

Article history:
Received 21 October 2023
Received in revised form 6 February 2024
Accepted 27 March 2024
Available online xxx

Keywords:
Lensless camera
Coded aperture imaging
Metasurface
Compressive sensing
Deep learning

ABSTRACT

Lensless imaging is an innovative and swiftly advancing technology at the intersection of optics, imaging technology, and computational science. It captures scene by directly recording the interference or diffraction patterns of light, subsequently utilizing algorithms to reconstruct the original image from these patterns. Lensless imaging transforms traditional imaging paradigms, offering newfound design flexibility and the capacity to seamlessly integrate within diverse imaging ecosystems. This paper aims to provide an overview of significant developments in optical modulation elements, image sensors, and reconstruction algorithms. The novel application scenarios that benefit from lensless computational imaging are presented. The opportunities and challenges associated with lensless camera are discussed for further improving its performance.

1. Introduction

Optical imaging is an old subject that arose from the desire of mankind to observe and record natural phenomena. As early as 400 B.C., Chinese philosopher Mozi addressed the phenomenon of small-aperture imaging in his book *Mo Jing* (Mohist Canon) [1]. Around 1400 years later, the medieval Arab scholar Alhazen chronicled his ideas on optics in *The Book of Optics* [2], which played a significant role during Europe's scientific and technological renaissance. In the middle of the 19th century, the next revolution occurred in optical imaging technique with the advent of photography, allowing humans to record and reproduce optical images. Kodak's launch of the first black-and-white digital camera in 1975 marked the inception of the digital imaging era. Since then, digital cameras have gained widespread attention following the development of computer technologies, allowing for the processing of optical images as digital signals. To this day, the design framework of an optical imaging system has been well-established, from the frontend hardware configuration to the postprocessing pipelines. The prevalent optical imaging model uses lenses to map the object onto the image sensor, achieving "what you see is what you get". However, the emerging needs in wearable / integrated sensors, internet of things, and augmented / virtual reality (AR/VR) have significantly driven the demand for miniaturized, multifunctional, and cost-effective imaging devices. Traditional lens-based cameras suffer from limitations such as low degrees of freedom in design, bulky sizes, high costs, and limited capabilities for multi-dimensional data acquisition. These constraints have hindered the further developments and applications of the existing imaging technology. Consequently, novel imaging models are actively explored to overcome these limitations.

Pioneering technologies have fostered the rise of computational imaging. The rapid evolution of computing capabilities has enabled researchers to push back the frontiers and opened doors to new fields such as image processing, computer vision, and deep learning [3]. Micro-/nanotechnology has made remarkable progress, leading to continuous enhancements in the performance of image sensors. These enhancements encompass improved resolution, signal-to-noise ratios, and dynamic ranges [4–6]. The collision of these research areas has driven the emergence and growth of computational imaging. Computational optical imaging technology models the entire imaging system from the standpoint of light propagation and information transmission. This modeling incorporates computing capabilities into the imaging system, enabling it to overcome the bottleneck of the well-established lens-based imaging systems [7].

Lensless imaging represents a burgeoning and pivotal domain within the realm of computational imaging. It harnesses advanced computational algorithms to reconstruct the scene directly from the raw mea-

* Corresponding author.
E-mail address: clc@tsinghua.edu.cn (L. Cao).

https://doi.org/10.1016/j.fmre.2024.03.019

Please cite this article as: S. Li, Y. Gao, J. Wu et al., Lensless camera: Unraveling the breakthroughs and prospects, Fundamental Research, https://doi.org/10.1016/j.fmre.2024.03.019

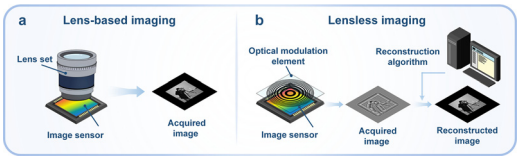

Fig. 1. Comparison between classical lens-based imaging and lensless computational imaging. (**a**) Schematic diagram of lens-based imaging. (**b**) Schematic diagram of lensless computational imaging.

surements, which are encoded by optical modulation elements instead of conventional lenses. This innovative approach has several advantages over traditional imaging methods, such as more flexibility, extended functionality, light weight and low cost. The advantages of lensless computational imaging have enabled breakthroughs in various fields including microscopy [8,9] three-dimensional (3D) imaging [10–12], multispectral imaging [13,14], light-field imaging [15] and digital holographic imaging [16–18].

In this paper, we present a comprehensive review of recent advancements in lensless computational imaging, with a particular focus on the three critical components of this technology: optical modulation elements, image sensors, and reconstruction algorithms. Over the past decade, significant progresses have been made in developing novel encoding elements for lensless computational imaging. Metasurfaces, in particular, have emerged as a promising alternative to traditional encoding elements that enables various functionalities with a compact setup. The principles behind these encoding elements and their applications in lensless camera are explored. The use of different types of image sensors in lensless camera is analyzed. We examine the most recent advancements in reconstruction algorithms, encompassing model-based techniques and deep learning-based methods. Various popular application scenarios where lensless imaging has demonstrated potential are examined, including microscopic imaging, multispectral imaging, 3D imaging, and optical fiber imaging. Alongside discussing the present state-of-the-art in lensless computational imaging, some of the pivotal challenges confronting this technology are pinpointed. We present strategies to address these challenges and enhance the performance of lensless camera. This paper provides a comprehensive overview of the incoherent imaging model in lensless imaging. The concepts and methodologies about the coherent lensless imaging [17,19–22] are not discussed in this paper.

2. Advantages of lensless computational imaging

Lens-based imaging has played a pivotal role in shaping the landscape of imaging technology. As represented in Fig. 1a, a conventional lens-based imaging system is characterized by the presence of a carefully arranged lens positioned in front of an image sensor. This optical configuration serves the fundamental purpose of capturing and conveying the light intensity faithfully to the sensor, forming the basis of many imaging applications. However, the rapidly evolving application scenarios have imposed greater demands on imaging devices, resulting in bottlenecks in traditional lens-based cameras. One of the key challenges lies in the heavy dependence of imaging performance on the system's size, weight, fabrication complexity, and cost. Furthermore, constrained by the underlying optical principles, lens-based imaging must cope with the trade-off between large field of view and a high spatial resolution, consequently restricting its imaging throughput. Capturing multidimensional data requires higher data bandwidth and longer acquisition time, which substantially increases the cost of data acquisition and transmission.

Unlike the traditional lens-based camera, the lensless camera, as depicted in Fig. 1b, embraces a fundamentally distinct approach. Instead of using composite optical lenses, it employs an optical encoding element positioned directly in front of the image sensor. Deviating from the conventional imaging paradigm, the captured sensor measurements are coded representations of the object to be imaged. By employing specific image restoration algorithms, these coded sensor measurements can be decoded and processed, leading to the faithful reconstruction of the target object.

By eliminating the dependence on optical lenses, lensless computational imaging systems yield several unique advantages. Lensless imaging gets rid of the dependence on bulky and complex optical lenses, allowing for miniaturization and integration of imaging systems. In contrast to their lens-based counterparts that use a series of lenses to form a point-to-point projection image on the sensor, lensless cameras obviate the need for the intricate arrangement of multiple lenses, thereby significantly reducing the physical size and simplifying the optical setup. The imaging systems are notably more compact, lightweight, and highly suitable for integration into portable or wearable devices.

Additionally, lensless imaging holds promise for overcoming the limitations in high-dimensional information encoding. The entire light field encompasses multiple dimensions, such as 3D spatial position, amplitude, phase, spectrum, polarization. When acquiring high-dimensional data, current imaging methods usually separate the signals to different dimensions and perform sequential measurements, leading to considerable time consumption. In contrast, lensless imaging encodes high-dimensional data into a two-dimensional (2D) intensity image, enabling optical compression of the image. Subsequently, optimization algorithms are employed to reconstruct the high-dimensional data from the 2D compressed measurement.

Lensless computational imaging effectively improves data acquisition efficiency, reduces hardware requirements, and facilitates real-time acquisition. By embracing the technology of lensless imaging, researchers can explore novel imaging paradigms and unlock new possibilities in data acquisition and analysis.

In practical application scenarios, a careful trade-off in the choice of imaging methods is still necessary [23–25]. Lens-based imaging systems have proven their effectiveness in many applications, demonstrating superior performance over lensless imaging in specific scenarios. For instance, well-designed multilevel diffractive elements can offer better optical performance and are relatively easy to fabricate [23,26]. Lensless imaging opens up new possibilities for ultra-thin, lightweight, and highly controllable optical system. It is crucial to consider the advantages and limitations of different imaging modes comprehensively for obtaining the outstanding imaging performance.

3. Key components of lensless computational imaging

Lensless computational imaging techniques enable the reconstruction of high-quality images from the sensor measurements, making it a promising tool for a wide range of applications [10,27–29]. A typical lensless computational imaging process is illustrated in Fig. 2. This imaging process comprises three crucial components: encoding optics, image sensor and decoding algorithm. The encoding optics perform physical coding of the target object with optical modulation elements, such as coded apertures and metasurfaces. The encoded intensity is then captured by the image sensor. The decoding algorithm utilizes advanced signal processing methods, such as compressive sensing and deep learning, to restore the target object from the raw measurement.

Within the framework of lensless computational imaging, optical modulation elements, image sensors and image reconstruction algorithms play pivotal roles in enabling advanced imaging capabilities. These essential components are crucial for achieving high-quality and efficient image reconstruction without the need for traditional lenses. In the following sections, we will delve deeper into the workings of optical modulation elements, explore various state-of-the-art image reconstruction algorithms, and introduce high-performance optical detection and processing chips.

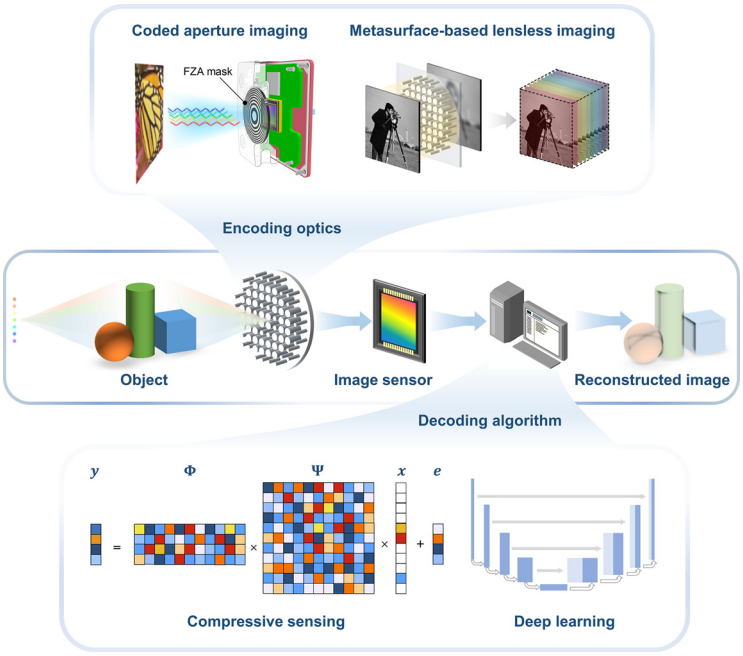

Fig. 2. Key components and imaging process of typical lensless computational imaging system. Key components: encoding optics, image sensor and decoding algorithm. During the imaging process, the information of object is encoded by encoding elements and captured by image sensors, after which the encoded information is decoded by reconstruction algorithms.

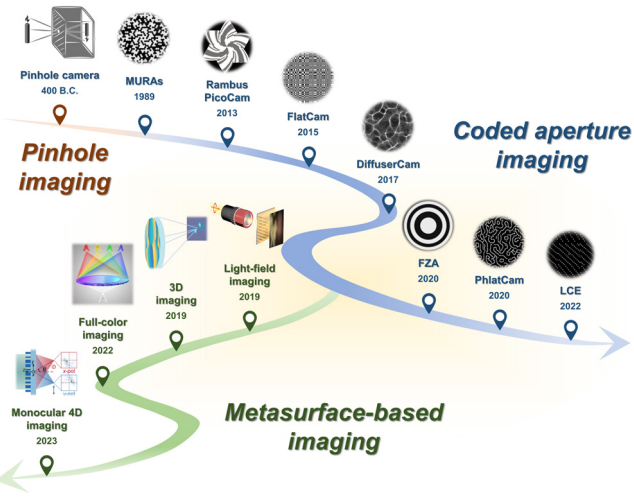

Fig. 3. Roadmap of optical modulation elements. Pinhole imaging is the earliest form of lensless imaging. Coded aperture imaging includes: MURA, 1989 [30]; Rambus PicoCam, 2013 [31]; FlatCam, 2015 [27]; DiffuserCam, 2017 [10]; FZA, 2020 [29]; PhlatCam, 2020 [8]; LCE, 2022 [32]. Metasurface-based imaging includes: light-field imaging, 2019 [33], 3D imaging, 2019 [34]; full-color imaging, 2022 [35]; monocular 4D imaging, 2023 [36].

3.1. Optical modulation elements

Fig. 3 illustrates a roadmap that traces the historical development of lensless imaging, highlighting key milestones in its evolution. The journey of lensless imaging commenced with pinhole imaging. As shown in Fig. 4a, pinhole imaging system involves capturing light through a tiny hole, allowing only a narrow beam of light to pass through and forming an image on the image plane. Although simple in its design, this early technique opened the door to new imaging possibilities. Building upon the principles of pinhole imaging, the technique of coded aperture imaging emerged as a significant breakthrough. As depicted in Fig. 4b, coded aperture imaging replaces the pinhole with a specially designed aperture in the light path. Compared with pinhole imaging, this approach enhances the system's efficiency and leads to improved image quality and resolution. The coded aperture can be classified as amplitude mask and phase mask. The amplitude mask modulates the amplitude of incident light by passing, blocking, or attenuating photons. The phase mask modulates the phase of incident light based on the principles of wave optics, changing the relative path-length in a 2D pattern. Compared to the amplitude mask, the phase mask exhibits higher transmission efficiency. More recently, the advent of metasurfaces has brought about a paradigm shift in lensless imaging. By exploiting light-matter interactions at sub-wavelength scale, metasurfaces possess extraordinary capabilities in manipulating light with precise control over their phase, amplitude, polarization, and dispersion. As illustrated in Fig. 4c, metasurfaces can be used to replace coded aperture as a more powerful information encoding device. Integrating metasurfaces as encoding elements in lensless imaging systems has opened up new avenues for capturing complex information from scenes with unprecedented functionalities.

Studying the manufacturing processes of optical modulation elements helps advance the further development of lensless imaging. Amplitude masks can be manufactured for a wide range of the working wavelength. In the fabrication process, a material capable of blocking light (e.g., Chromium) is typically deposited onto a transparent substrate. A photolithography process is employed to create the mask pattern [9,29]. Phase modulators can be manufactured by photolithographically etching patterns or through an additive process of controlled polymerization of photoresist on the transparent substrate. The fabrication methods for metasurfaces can be broadly categorized into three types: direct-write lithography, nano-imprint lithography, and hybrid patterning lithography [37]. To realize cost-effectiveness, high throughput, high repeatability, and high resolution in fabrication, there is a need to refine existing techniques and advance the developments of fabrication methods.

3.1.1. Coded aperture

Coded aperture imaging is founded on the principles of pinhole imaging, a fundamental lensless imaging technique that has been explored

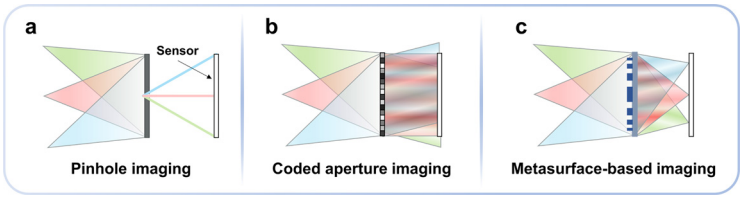

Fig. 4. The comparison of pinhole imaging, coded aperture imaging and metasurface-based imaging. (**a**) Pinhole imaging. (**b**) Coded aperture imaging. (**c**) Metasurface-based imaging.

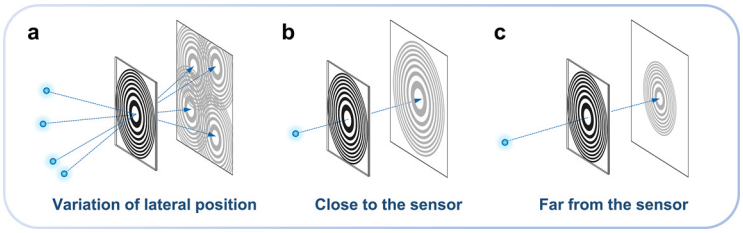

Fig. 5. The encoding principle of a coded aperture lensless camera for 3D imaging. (**a**) Lateral position is encoded by the displacement of the PSF. (**b, c**) Depth position is encoded by the magnification of the PSF.

since ancient times. The resolution of a pinhole camera is heavily dependent on the aperture size. This is because the pinhole is a finite-size aperture, not a geometric point. Light emitted from object points, after passing through the pinhole, forms a divergent light beam, resulting in spots on the image plane instead of points. Overlapping of these spots leads to the image blur. When there is no overlap between two spots, the corresponding two object points can be considered resolvable. From the perspective of geometric optics, the resolution of the pinhole camera can be expressed as $\Delta r = d(1 + u/v)$. Here, Δr represents the minimum resolvable distance on the object plane, d is the pinhole diameter, u denotes the object distance, and v is the image distance. Reducing the aperture size could enhance the resolution of pinhole imaging. However, smaller apertures lead to a lower light efficiency, a reduced signal-to-noise ratio, and increased diffraction effects, resulting in noisy and low-quality images. Pinhole cameras are rarely used in the visible regime but have found their applications in high-energy imaging owing to their robustness against high-energy rays [38–40].

Coded aperture imaging has gained substantial attention within the realm of lensless imaging. By replacing optical lenses with a thin and flat mask, the weight and size of the imaging system can be significantly reduced. In coded aperture imaging system, a coded mask with specific pattern is placed in front of the image sensor, which defines the point spread function (PSF) of the imaging system. The picture captured by the image sensor is no longer a direct representation but instead an encoded pattern of the scene. The scene can be eventually obtained by utilizing reconstruction algorithms. The imaging process from the target scene to the raw measurement can be expressed as a linear system, whose parameters are determined by the pattern and position of the mask. As an example, we consider a coded aperture shown in Fig. 5, where point sources are placed in front of the coded aperture. In this scenario, the image sensor captures the projected pattern of the mask. When the lateral position of the light source is altered, the projected pattern on the image sensor shifts accordingly (Fig. 5a). Similarly, changing the depth of the light source alters the size of the projected pattern (Fig. 5b, 5c).

The first proposed coded aperture was the Fresnel zone plate (FZP). In 1950, Rogers observed the similarities between FZP and point source hologram, which he considered as a generalized zone plate with complex patterns [41]. In 1961, Mertz and Young proposed to use FZP as an encoding aperture, which could be employed under incoherent illumination to obtain a coded image similar to a gabber hologram [42]. And then the coded image could be decoded through optical reconstruction. This method, also known as zone plate coded imaging, finds widespread use in astronomy, nuclear medicine, and laser inertial confinement fusion. In 1968, Dicke and Ables independently proposed random aperture arrays for X-ray and gamma-ray imaging [39,40]. Subsequently, non-redundant arrays (NRA) [43], uniformly redundant arrays (URA) [44], and modified uniformly redundant arrays (MURA) [30] have been proposed successively.

In recent years, significant advancements have been made in coded aperture imaging with respect to encoding models, mask design, and reconstruction algorithms. A notable example of a coded aperture lensless camera is the PicoCam, designed by Rambus in 2013 [31]. It utilizes a spiral phase grating to achieve broad-spectrum imaging. In 2015, Asif et al. introduced the FlatCam, which was designed based on a separable mask [27]. The separable mask pattern is constructed by performing the inner product of two one-dimensional vectors, which significantly reduces the computational complexity of the measurement matrix, thereby enabling scalable calibration and image reconstruction. Another approach to coded aperture imaging is the DiffuserCam, which was developed by Antipa et al. in 2017 [10]. This camera utilizes a scattering layer and requires pre-experiment calibration to obtain the PSF patterns at different depths, each approximated as a linear system with spatial translational invariance. In 2020, Wu et al. proposed FZA lensless camera, a novel approach to coded aperture lensless imaging that supports high-quality imaging without the need for strict calibration [29]. In the same year, Boominathan et al. proposed the PhlatCam, which features a high-performance contour-based PSF [8]. In 2022, Zhang et al. proposed a lensless compound eye (LCE) microsystem capable of achieving a wide field of view, high resolution, and high update rate [32]. The micro-lens array is an important type of coded aperture. This camera dispenses with the main bulky lens and is composed of only one layer of microlens array and the image sensor. When combined with reconstruction algorithms, camera using micro-lens array can achieve 3D microscopic imaging [45,46].

Typical encoding masks are illustrated in the roadmap of Fig. 3 [8,10,27,29–32]. Each of these masks corresponds to different PSF, playing a critical role in determining the resolution and quality of the reconstructed image. There are studies on the design of encoding masks based on the PSF, achieving wide spatial frequency support [8,47]. Other works take into account the constraints of manufacturing costs. DiffuserCam employs inexpensive diffusers to achieve high-quality image reconstruction [10]. Certain encoding mask designs offer simplicity and ease of adjustment. FZA, for instance, enables high-quality imaging without the need for strict calibration [29,48]. These

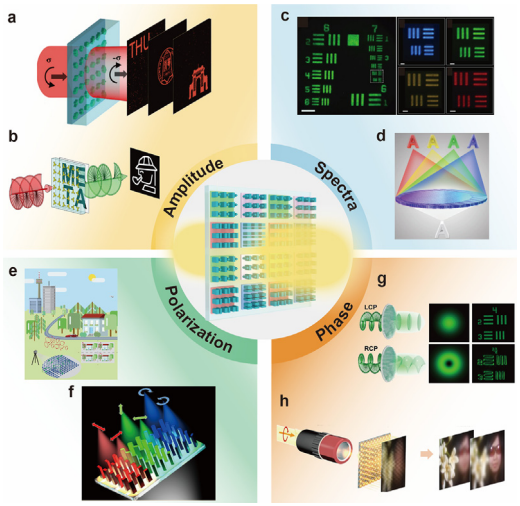

Fig. 6. Various degrees of freedom for light control provided by metasurfaces. (**a**) An ultra-thin metasurface that can arbitrarily modulate the complex amplitude [50]. (**b**) The amplitude of second harmonic waves modulations achieved by a nonlinear plasmonic metasurface [55]. (**c**) The TiO_2 visible-range metalenses provide diffraction-limited focal spots at arbitrary design wavelengths. The diffraction-limited focusing is demonstrated at wavelengths of 405, 532, and 660 nm [56]. (**d**) The transversely dispersive imaging of metalens which can resolve spectral information [57]. (**e**) A compact full-Stokes polarization camera [51]. (**f**) Polarimetric imaging based on polarization multiplexed metalenses [58]. (**g**) Fourier transform setup for switching between bright-field imaging and phase contrast imaging modes [59]. (**h**) Light-field imaging with GaN metalens array [33].

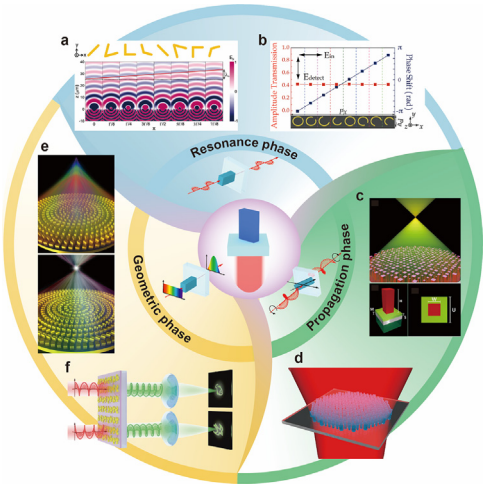

Fig. 7. Phase modulation techniques for metasurfaces. (**a**) Phase manipulation with V-antennas [60]. (**b**) A linear phase profile of a 2π range is obtained using C-shape split-ring resonator [62]. (**c**) An achromatic metalens operating over a continuous bandwidth in the visible, the phase shifter is TiO_2 nanopillar with a square cross-section [64]. (**d**) High numerical aperture metalens is achieved by using circular nanopillars [65]. (**e**) Chromatic and achromatic metalenses based on metasurface [66]. (**f**) Nonlinear chiroptical holography with PB phase controlled plasmonic metasurface [53].

works signify the development of coded aperture imaging, making lensless imaging a hotspot for advanced imaging research.

3.1.2. Metasurface

Metasurfaces are composed of nanostructures with a feature size much smaller than the wavelength. These subwavelength meta-atoms are capable of modulating various properties of light, including phase [49], amplitude [50], spectrum [13], polarization [51,52], hologram [53] and angular momentum [54], making it an effective encoding element in imaging systems. Three-dimensional image can be reconstructed from a complex-amplitude computer-generated hologram. The ultrathin dielectric metasurface is used to controlled amplitude by tuning the geometric size of the meta-atom (Fig. 6a) [50]. The real space and the holographic images are simultaneously encoded by using a nonlinear diatomic metasurface. The amplitude modulation is achieved by the interference between the second-harmonic generation (SHG) waves in a meta-molecule (Fig. 6b) [55]. The metalenses at visible wavelengths with efficiencies as high as 86 % were demonstrated. They have high numerical apertures (NA) of 0.8 and are capable of focusing light into diffraction-limited spots (Fig. 6c) [56]. Based on the transversely dispersive TiO_2 metalens, the ultra-compact spectral light-field imaging (SLIM) that can simultaneously resolve 3D spatial information and spectral information is proposed. Using white light illumination, the letter is imaged by the metalens to different positions at different wavelengths. (Fig. 6d) [57]. Metasurface-based full-Stokes compact polarization camera without conventional polarization optics or moving parts is designed, which provides a simplified route for polarization imaging (Fig. 6e) [51]. The dielectric metasurface contains three metalenses designed with two orthogonal polarization dependences can correctly measure the polarization state for different input polarizations (Fig. 6f) [58]. A spin-multiplexed metasurface-based optical imaging system was proposed and demonstrated. The metasurface spatial filter formed by TiO_2 nanopillars could provide two uncorrelated phase profiles corresponding to the spin states of the incident light (Fig. 6g) [59]. By combining geometric phase and dynamic phase, light-field images with a polarization-dependent achromatic GaN metalens array were designed, which clearly demonstrated multidimensional optical information, including full-color imaging and depth (Fig. 6h) [33]. Metasurface-based optical components have the potential to fulfill the demand for miniaturization of instruments, leading to reduced size, weight, and power consumption of optical systems. This attribute is particularly advantageous for emerging technologies like internet of things, autonomous driving, wearable devices, AR/VR, and remote sensing.

Metasurfaces can be classified into three types based on phase modulation techniques: resonance phase metasurface, geometric phase metasurface, and propagation phase metasurface. Resonant phase modulation entails achieving a phase shift through variations in the resonant frequency that is controlled by the meta-atom's geometry. Geometric phase modulation achieves phase shift by adjusting the rotation angle of meta-atoms. Propagation phase modulation controls the phase by manipulating the optical path length difference generated during light propagation. These different types of phase modulation techniques provide flexibility and versatility in designing and implementing metasurface-based encoding elements.

Most of the initial investigations on metasurfaces have focused on resonance phase modulation. Resonance phase metasurfaces achieve the desired phase modulation by leveraging the dispersion characteristics of subwavelength metallic antennas. These antennas can be regarded as optical resonant structures, generating a displacement current in the structure when the incident light is tuned close to their resonant wavelength. This results in a strong scattered electromagnetic field, where a significant change in the phase shift between the scattered and incident light occurs during the resonance. Altering the geometry of the resonant structure provides a means to achieve the desired phase shift on the metasurface. In 2011, Capasso's group proposed a V-shaped antenna for metasurface. By varying the arm length and angle of the V-shaped antenna, they successfully achieved continuous variation of the phase from 0 to 2π (Fig. 7a) [60]. In the same year, Sun et al. designed an H-shaped resonant metasurface, achieving the conversion of propagating waves to surface waves in microwave band [61]. Zhang, Liu et al. proposed the C-shape metasurface in 2014 (Fig. 7b) [62,63]. These research findings

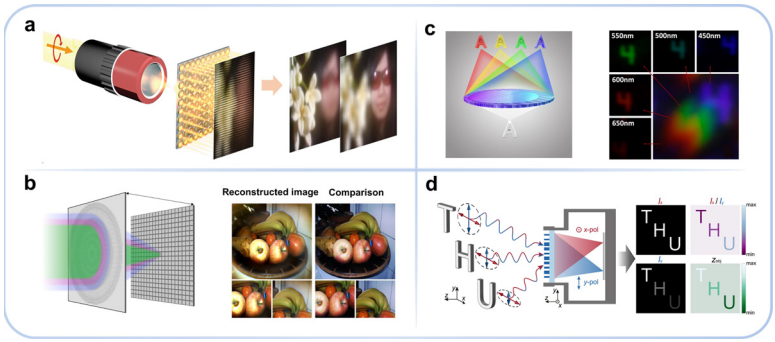

Fig. 8. Computational imaging based on metasurface. (**a**) Metalens array for light field imaging [33]. (**b**) Full-color, low-dispersion, wide field-of-view imaging achieved by combining a metalens with neural network algorithm [35]. (**c**) Metalens-based spectral light-field imaging [57]. (**d**) Monocular camera which can perform both depth sensing and polarization imaging with exceptional accuracy [36].

have opened up new avenues for the application of metasurfaces in flat optics.

Propagation phase metasurfaces consist of 2D arrays of meta-atoms with high refractive index contrast. It manipulates the phase by the optical path difference generated during the propagation of electromagnetic waves. Assuming the wavelength of an electromagnetic wave is λ, the cumulative propagation phase ϕ of an electromagnetic wave propagating at a distance d in a medium with an effective refractive index n can be expressed as $\phi = (2\pi/\lambda)$. Adjusting the phase shift necessitates spatially modulating the period and physical parameters of each meta-atom [67]. Achromatic metalens, which focus the incident light at the same focal plane in a continuous and wide range of wavelength is demonstrated. The desired phase coverage is obtained by varying a geometric parameter (Fig. 7c) [64]. In 2018, Fan et al. employed the propagation phase design method to create a large-aperture SiN metalens with a high numerical aperture (Fig. 7d) [65].

Geometric phase, also known as Pancharatnam-Berry (PB) phase, is a phenomenon in which changes in the polarization state of light are related to the trajectory of the Poincaré sphere change process. In 1956, Pancharatnam discovered this relationship between phase and polarization when multiple changes occur [68]. In 1984, Berry proposed that an eigenstate of a quantal system acquires a phase factor linked to the geometrical path when it undergoes an adiabatic cycle [69]. In the linear optical regime, combined the integrated-resonant unit element in metasurfaces with smooth and linear phase dispersion with geometric phase to design broadband achromatic flat optical components is proposed (Fig. 7e) [66]. In nonlinear optics, the chiroptical holography is achieved by combining the giant circular dichroism in SHG effect and the theory of nonlinear Pancharatnam–Berry (PB) phase on plasmonic metasurface (Fig. 7f) [53]. PB phase, which corresponds to the additional phase difference introduced by the path between two points on the Poincaré sphere, is equal to twice the in-plane orientation angle of each meta-atom. By altering the orientation angle of meta-atoms, phase shifts occur in electromagnetic waves, which allow for artificial control of the phase [70]. This greatly reduces the design and processing complexity of metasurfaces.

Recently, researchers combined the light field modulation capability of metasurface with computational imaging methods, presenting new opportunities for lensless computational imaging. By introducing metasurface, the complexity of the imaging system can be significantly reduced. Lensless imaging based on metasurface encoding has made significant progress in various fields, including light field imaging, full-color imaging, spectral imaging, and 3D imaging. In 2019, Lin et al. achieved full-color light field imaging based on an achromatic planar metalens array combined with a light field rendering algorithm [33] (Fig. 8a). In 2020, Park et al. proposed an electrically controlled virtual-moving metalens array, which circumvents the trade-off between the spatial and angular resolution pertaining to the light field imaging [71]. In 2021, Tseng et al. used an agent function to replace the phase distribution of a metalens [35] (Fig. 8b). Through continuous iterations and improvements in deep learning and image reconstruction algorithms, full-color, low dispersion, wide field-of-view imaging based on a metalens was successfully achieved. In 2022, Hua et al. demonstrated a four-dimensional (4D) imaging technique based on a metalens, which can realize the combination of 3D imaging and spectral imaging [57] (Fig. 8c). In the same year, Jing et al. proposed a metasurface-based single-shot 3D imaging technique, which achieved a remarkable reconstruction accuracy of 0.3 mm at a measuring distance of 300 mm [72]. Recently, in 2023, Shen et al. proposed a monocular camera that can achieve single-shot 4D imaging with high precision and fidelity [36] (Fig. 8d). The point-spread functions of metalens are highly dependent on the depth of the target object. By combining the camera with image retrieval algorithms, the system can perform both depth sensing and polarization imaging with exceptional accuracy simultaneously over an extended depth of field. Metasurfaces still encounter challenges in terms of efficiency, dispersion, and fabrication, with the overall performance remaining behind that of traditional lenses. Accordingly, it is crucial to undertake a meticulous investigation into the advantages offered by metasurfaces as a substitute for traditional lenses.

3.2. Image reconstruction algorithms

In contrast to traditional lens-based imaging, which follows the principle of "what you see is what you get", lensless imaging systems incorporate the unique design strategy to enhance the connection between the adopt indirect measurements from which the target scene is barely visible. Reconstruction algorithms are developed to retrieve the target scene faithfully from the raw measurement. The accuracy and efficiency of these algorithms are critical elements in obtaining high-quality images in lensless imaging systems.

For incoherent lensless imaging, the desired signal usually corresponds to the intensity distribution in certain dimensions. The imaging process, i.e., the mapping from the target scene into the coded image, can be represented by a linear operator as [73],

$$\mathbf{b} = \mathbf{\Phi} a + \mathbf{e}, \tag{1}$$

where $\mathbf{a} \in \mathbb{R}^N$ is an N-dimensional vector representing the intensity of the target scene, $\mathbf{\Phi} \in \mathbb{R}^{M \times N}$ is the measurement matrix, with each column vector representing the response of the sensor to a spatial point, $\mathbf{b} \in \mathbb{R}^M$ represents the measurements captured by the image sensor, and $\mathbf{e}$ accounts for the measurement noise. Given the measurement matrix $\mathbf{\Phi}$, recovering $\mathbf{a}$ from $\mathbf{b}$ is a classical linear inverse problem. Despite challenges posed by model errors, system noise and the ill-posed nature of many image reconstruction problems (with $M \ll N$), efforts have been made to address the difficulties with the help of advanced signal processing techniques.

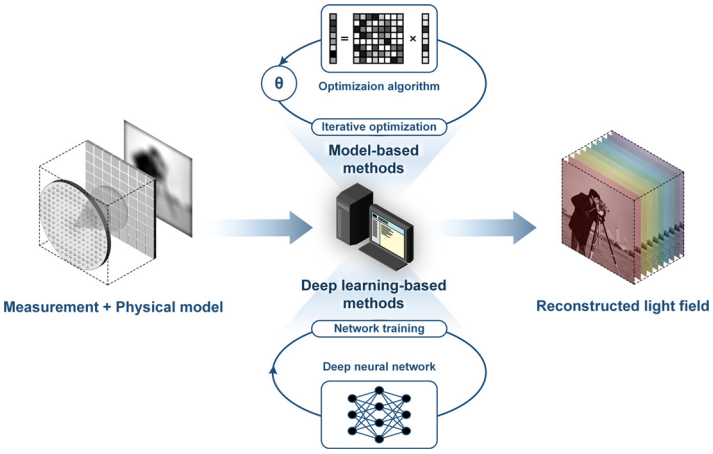

Fig. 9. The general pattern of the lensless imaging reconstruction algorithms. The reconstruction algorithms can be broadly categorized into model-based optimization methods and deep learning-based methods.

Various approaches have been proposed for image reconstruction, which can be categorized into two main types: model-based optimization methods and deep learning-based methods. A general framework of the reconstruction algorithms for lensless imaging is illustrated in Fig. 9. Model-based algorithms recast image reconstruction as an optimization problem. A typical objective function penalizes deviation from the forward model, incorporating prior knowledge and assumptions about the target scene. A solution to the problem can be found with a properly tuned iterative solver. The target scene can be accurately retrieved when the forward model and prior assumptions are satisfied. Deep learning-based algorithms sidestep the explicit modeling of the physical system and priors, and learn the implicit inverse mapping from large amounts of training data. By leveraging the advancement in parallel computing, deep learning-based algorithms have the capability to perform real-time inference on large-scale data.

3.2.1. *Model-based methods*

In model-based approaches, image reconstruction is typically reformulated as a numerical optimization problem, which can then be solved by off-the-shelf algorithms. When solving inverse problems for lensless imaging, several technical challenges are commonly encountered. Ill-posedness is a typical characteristic, because the measurement schemes usually correspond to down-sampling operators from high-dimensional space. Prior knowledge is required to ensure uniqueness of the solution and improve stability of the solvers. The measurement noises can also impact the solution to the inverse problems, leading to reduced reconstruction quality. Therefore, proper noise modeling and suitable denoising methods are crucial factors in addressing the inverse problem. Data incompleteness arises when certain sensor measurements are missing or inaccessible, thereby increasing the complexity of the inverse problem. To complete the missing information, techniques such as interpolation, extrapolation, or data compensation can be employed. When solving particular inverse problems, high-performance computing devices or efficient algorithms are greatly demanded. To tackle the aforementioned challenges, researchers aspire to discover image reconstruction methods that exhibit high accuracy, robustness, and computational efficiency.

Based on the above considerations, the general formula for model-based lensless imaging reconstruction is given by

$$\min_{\mathbf{a}}\{F(\mathbf{a})+\tau\mathfrak{R}(\mathbf{a})\}, \tag{2}$$

where $F(\mathbf{a})$ denotes the data-fidelity term that enforces model consistency according to Eq. (1). A typical choice is the squared error $\|\mathbf{\Phi}a-\mathbf{b}\|_2^2$, which corresponds to the maximum likelihood estimation under additive white Gaussian noises. $\mathfrak{R}(\mathbf{a})$ denotes the regularization term and τ is the parameter controlling the weight of $\mathfrak{R}(\mathbf{a})$. The regularization term imposes prior knowledge and penalizes false ambiguous solutions. Common regularization techniques include Tikhonov regularization and sparsity regularization. The minimization problem can be solved via standard optimization algorithms such as the iterative shrinkage thresholding algorithm (ISTA) [74], two-step iterative shrinkage thresholding (TwIST) [75], fast iterative shrinkage thresholding algorithm (FISTA) [76], and alternating direction method of multipliers (ADMM) [77]. These algorithms iteratively update the image estimates with respect to the fidelity term and the regularization term, thereby progressively enhancing the reconstruction results.

In classical lensless imaging, sparsity-based regularization techniques have been widely explored to improve the reconstruction quality. For example, in FlatCam and FZA imaging, considering that most natural scenes exhibit piece-wise smoothness and typically have sharp edges, gradient-domain sparsity has been utilized to regulate the inverse problem [27,29,78,79].

Model-based methods benefit from the high interpretability due to the explicit representation of the physical models and signal priors. However, accurate modeling of real-world scenarios can be technically challenging or computationally demanding, making it infeasible in practice. Handcrafted priors are also limited in terms of expressiveness. Consequently, the reconstruction quality remains far from optimal. Furthermore, the iterative nature of reconstruction algorithms renders them time-consuming and unsuitable for real-time applications. It becomes imperative to explore more advanced algorithmic decoding techniques for lensless imaging.

3.2.2. *Deep learning-based methods*

Deep learning is a computational approach that employs multiple neurons as its fundamental units, consisting of input and output layers, along with hidden layers. This enables the characterization of intricate models through a multitude of nonlinear operations and learnable parameters. It learns the implicit features embedded with the training data, which serves as the prior knowledge for the inversion of the problem. Deep learning also offers innovative solutions to inverse problems. In recent years, deep learning has gained attention in lensless computational imaging. Compared to iterative optimization methods, data-driven deep learning methods have the advantages of better robustness, higher reconstruction quality, and faster or even real-time inference and computation using high-performance graphics processing units.

In the field of lensless imaging, numerous prevalent neural networks find application including fully connected neural networks (FCNNs) [80,81], convolutional neural networks (CNNs) [82,83], and transformer [84]. In recent years, more advanced deep learning-inspired algorithmic frameworks have been introduced into the context of lensless

imaging. In 2017, Sinha et al. pioneered the application of deep neural networks (DNNs) to address end-to-end inverse problems in computational imaging [85]. In 2019, Monakhova et al. employed algorithm unrolling technique within the alternating direction method of multipliers (ADMM) framework. The resulting algorithm, when combined with a U-net for further refinement, outperformed the traditional ADMM algorithm in terms of perceptual quality and reconstruction speed [86]. In 2020, Khan et al. proposed FlatNet, which consists of a physical inversion step and a U-net architecture for image quality enhancement. When trained with experimentally collected dataset, the algorithm can achieve photorealistic recovery of real scenes [87]. Based on the previously developed FZA lensless camera, Wu et al. proposed to use a U-net for inversion and a deep back-projection networks (DBPN) [88] for image quality enhancement, which achieved a speedup of two orders of magnitude compared with traditional iterative algorithms, while realizing competitive reconstruction quality after training on a simulated dataset [89]. Zhou et al. carried out an in-depth study on deep learning reconstruction methods for lensless imaging and proposed learned analytic solution net (LAsNet), which combines physical imaging models with deep learning to achieve high-quality image reconstruction [90]. They proposed a neural network with a deep noise prior for the FlatCam image reconstruction [91].

In the training process of neural networks, datasets are indispensable and can be categorized into real and synthetic data. Real data is directly collected or measured through experiments. However, due to the limited number of samples, high collection costs, and long acquisition time associated with real data, synthetic data has become widely used. Synthetic data, generated by computer simulation or algorithms, can be used as a substitute for real data [92]. Using synthetic data reduces the necessity of collecting real data, thus enabling faster construction and lower costs. Wu et al. utilized a synthetic dataset for training neural networks [89]. The training data was generated using a diffraction model based on the DIV2K dataset [93], eliminating the need for laborious collection of real images. The reconstructed results showed improved reduction in blur caused by diffraction. The computational speed has two orders of magnitude faster than that for traditional iterative image reconstruction algorithms. The performance of a neural network may heavily rely on training datasets. Therefore, comprehensive consideration of factors such as task requirements, choice of generation models, data diversity, and authenticity is essential when constructing synthetic datasets to ensure the neural network performs well.

Deep learning can also be used for the design of the imaging components. Hardware and algorithm can be jointly designed, thereby further improving the sampling efficiency and reconstruction quality. In 2020, Horisaki et al. applied deep learning to mask design [94]. The scene image was convolved with the encoded aperture, serving as the convolution layer of the neural network, while the mask pattern functioned as a learnable parameter. The concurrent training of the imaging simulation network and the image reconstruction network enabled simultaneous achievement of mask design and high-quality reconstruction. In 2016, the design of end-to-end imaging systems based on diffractive optical elements has been realized for various computational imaging applications [95–97]. Later in 2021, Tseng et al. designed a nano-optic camera, replacing the bulky lens set with an extremely thin metasurface [35]. The polynomial coefficients that determine the phase of the metasurface were utilized as trainable parameters, along with a feature-based deconvolution algorithm, resulting in imaging quality comparable to that of a conventional lens-based camera.

3.3. Optical detection and processing chips

Optical detection and processing chips are electronic devices that convert light signals into digital images, operating based on the principle of the photoelectric effect. These sensors consist of an array of photosensitive elements that individually detect the intensity of light. These photosensitive elements accumulate charge at each pixel, forming a charge pattern corresponding to the captured image. The sensor reads and digitizes these charges into voltage signals, which are then converted into digital signals via an analog-to-digital converter for computer processing. Image sensors, such as CCD (Charge-Coupled Device) and CMOS (Complementary Metal-Oxide-Semiconductor) sensors, are widely used in digital cameras, smartphones, and various other imaging devices.

In the realm of lensless imaging, achieving high-quality results relies not only on optical modulation and sophisticated algorithms but also on the capabilities of the sensor. The capabilities of sensor can greatly influence the effectiveness and quality of lensless imaging techniques. As shown in Fig. 10, lensless imaging sensors require higher pixel resolution and larger dynamic range to achieve optimal performance. Integrating them with optical components can reduce the overall size of the imaging system. Additionally, researching in-sensor and near-sensor computing techniques can help overcome the limitations associated with traditional information processing architectures. In forthcoming developments, innovative sensor technologies may potentially revolutionize the field of lensless imaging by pushing the boundaries of what is currently achievable. It holds the promise of offering new possibilities and applications for lensless imaging technology.

In lensless computational imaging system, the quality of the reconstruction image is susceptible to the noise and signal errors of detectors. To achieve accurate reconstruction results, photodetectors with higher pixel resolution and larger dynamic range are necessary. Nevertheless, as the pixel pitch decreases, the crosstalk between adjacent pixels increases, introducing errors in image reconstruction. Therefore, inter-pixel crosstalk suppression becomes an important issue in high-density detector research. In 2012, Toshiba Electronics embarked on studying deep trench isolation (DTI) technology for reducing the pixel crosstalk in CMOS image sensors (CIS) [98]. In 2021, Samsung Electronics reported a full-depth trench isolation (FTI) technique for a 32-megapixel CIS, achieving a pixel pitch of 0.64 μm [103]. The FTI technique can significantly minimize inter-pixel crosstalk and reduce signal errors in image reconstruction. Lensless computational imaging demands superior performance of the photodetectors, with the dynamic range as another key parameter to consider. In 2019, Chiou et al. achieved a dynamic range of 141 dB using adaptive multi-stage sampling [99]. However, increasing the dynamic range may lead to poor linearity. To address this issue, Leñero-Bardallo et al. proposed an asynchronous event-based overflow detection mechanism, which reduced nonlinearity to 3.5 % at 105 dB at frame rate of 30fps while eliminating distortion caused by pixel self-resetting [104].

Beyond the realms of high resolution and large dynamic range, the integration of optical components and optoelectronic chips plays a critical role in determining the miniaturization and integration of lensless computational camera. By integrating well-designed artificial structures, sophisticated optical responses can be achieved, thereby creating novel opportunities for crafting compact optical devices. In 2023, Zhang et al. proposed a tens-of-megapixel handheld multi-spectral camera [100]. They fabricated a structured thin film capable of executing multiplexed wavelength-dependent encoding. The thin film can be mounted onto the bare sensor directly by using a fiber optic plate to achieve a lightweight acquisition system. Apart from traditional structed film, metasurfaces can also be integrated with optoelectronic devices to improve imaging quality. Zuo et al. reported a chip-integrated metasurface-based polarimetric imaging sensor, which is realized by integrating an ultrathin metasurface onto a sensor with CMOS compatible fabrication processes [105].

Image reconstruction quality in lensless cameras is profoundly influenced by the computational capability. Computing blocks in or near optoelectronic sensor can reduce massive redundant data, subsequently alleviating both power consumption and response time in data transmission. Efforts could be made to explore novel computing architectures to address this challenge. In-sensor computing and near-sensor computing have emerged as breakthrough solutions that overcome the limi-

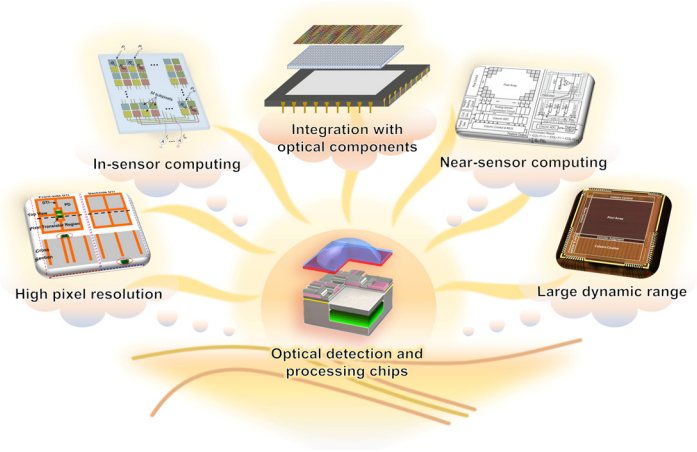

Fig. 10. Future directions for optical detection and processing chips. Lensless imaging sensors require high pixel resolution [98] and large dynamic range [99]. The size of the imaging system can be reduced by integrating image sensors with optical components [100]. In-sensor [101] and near-sensor [102] computing techniques enable effective raw data processing within or near the detector.

tations of traditional information processing architectures. These approaches enable effective raw data processing within or near the detector. These techniques improve computing capability, minimize redundant data transmission, and are highly integrated, making such approaches a hot topic in the development of photodetector and computational processing technologies [106,107].

In terms of in-sensor computing, in 2020, Mennel et al. reported a neural network photodetector that can simultaneously sense and process optical images without latency [101]. In 2021, based on a novel neural network, Zhang et al. reported an all-in-one device fused with sensing, storage, and computing capabilities [108]. However, current image sensors lack the capability for complex algorithms like image reconstruction. Near-sensor computing has higher energy efficiency and greater integration, and can support more complex algorithms. In 2019, Tang et al. proposed the fundamental architecture that realizes low-power deep learning accelerators within image sensors [102]. In the same year, Kim et al. proposed an analog-digital hybrid image processor for artificial intelligence that offers DNN accelerated computations with an ultra-low-power consumption of 0.62 mW [109]. In 2020, Chen et al. proposed an ADC-free near-sensor processing architecture that enables convolutional computation in the mixed-signal domain [110]. This ADC-free processing architecture has up to 545.4 GOPS/W energy efficiency with 1.8 mW power consumption. In 2021, Hsu et al. reported a real-time computational image sensor architecture that supports programmable convolution kernels, enabling real-time image detection and computational recognition at frame rates up to 480 Hz with FoM as low as 9.8 pJ/pixel/frame [111]. These novel computational architectures have broken through the limitations of traditional information processing architectures, providing innovative solutions for the photodetectors in lensless imaging.

4. Selected applications

The advancement of lensless imaging has led to diverse applications across various fields. This section aims to introduce the applications of lensless imaging, highlighting its advancements in the fields of microscopic imaging, multispectral imaging, 3D imaging, and optical fiber imaging, as illustrated in Fig. 11.

4.1. Microscopic imaging

Microscopic imaging systems have limited resolution due to diffraction limit and the complex imaging environment. Consequently, the exploration of new imaging techniques is essential. Lensless computational imaging has the advantages of large field of view, high resolution, and excellent portability, which is widely used in microscopic imaging. Empowered by super-resolution algorithms, lensless imaging has revolutionized microscopic imaging by eliminating the diffraction limit, making it a highly promising imaging method. With these benefits in mind, lensless microscopic imaging has found applications in diverse fields, including disease screening, environmental monitoring, and cellular dynamic monitoring. Through the years, researchers have made significant strides in the development of lensless microscopic imaging. In 2008, Seo et al. successfully applied lensless imaging to on-chip cytometry, achieving high-throughput automatic sorting of mixed solutes of red blood cells, yeast cells, E. coli, and various sized micro-particles [114]. In 2010, Zheng et al. utilized a pixel super-resolution algorithm to achieve a limiting resolution of 0.75 μm. This resolution is beyond the limit of 3.2 μm for image sensor pixel size [115]. In 2017, Adams et al. proposed FlatScope lensless microscopy to achieve 3D fluorescence imaging with micrometer resolution [9]. In 2018, Tønnesen et al. proposed a novel brain tissue cell microscopy based on super-resolution shadow imaging (SUSHI). It combines shadow imaging with super-resolution fluorescence imaging, which can visualize brain tissue with a resolution of up to the order of 10 nm (Fig. 11a) [112].

In addition to high resolution, microscopy also requires a large field of view. Metasurfaces offer opportunities for compact, thin, and lightweight wide-angle imaging. In 2019, Nakamura et al. designed a super field of view lensless camera which is composed of multiple coded image sensors, achieving a field of view of up to 180° [116]. In 2022, Chen et al. proposed a planar wide-angle-imaging camera that utilizes a metalens array [117]. In this work, researchers designed a one-dimensional metalens array that integrates with a CMOS image sensor. Each metalens can image incident light from a certain range of angles, and these sub-images are stitched together to form a full wide-angle image. They achieved wide-angle imaging with a range of over 120°. In the same year, Zhang et al. proposed a lensless compound eye (LCE) microsystem capable of achieving a wide field of view, high resolution, and high update rate [32].

4.2. Multispectral imaging

Multispectral imaging is an effective tool for capturing spectral information to facilitate target identification and analysis. Traditional spectral imaging systems commonly employ spectrometers to acquire spectral information at different wavelengths. However, the development of conventional spectrometer is limited by their bulky size and high cost. These spectrometers suffer from low information collection efficiency. Spectral imaging based on a lensless imaging system encodes incoming light spatio-spectrally by introducing a specific diffraction

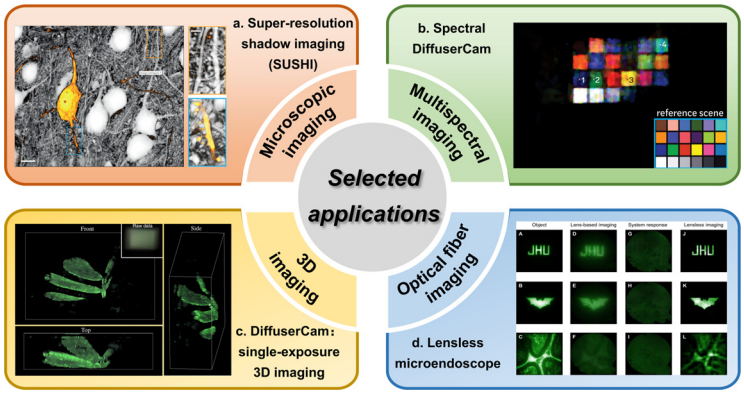

Fig. 11. Selected applications. (**a**) Microscopic imaging: a novel brain tissue cell microscopy based on SUSHI [112]. (**b**) Multispectral imaging: a high-resolution snapshot hyperspectral lensless imaging technique based on Spectral DiffuserCam [13]. (**c**) 3D imaging: a single-exposure 3D imaging system based on DiffuserCam [10]. (**d**) Optical fiber imaging: a randomly encoded mask positioned at the end of an optical fiber to build a lensless microendoscopic system [113].

structure to the optical system, enabling the recovery of spectral information through reconstruction algorithms. This approach simplifies the system structure, resulting in a more compact optical system. In 2020, Monakhova et al. proposed Spectral DiffuserCam, which enabled high-resolution snapshot hyperspectral lensless imaging with a spectral filter array (Fig. 11b) [13]. In 2021, Wang et al. developed a lensless imaging-based multispectral camera utilizing multispectral coded aperture [14]. The transverse chromatic aberration can enhance the extraction of spectral information significantly. In 2022, by dispersing light of different wavelengths in the same image plane, Hua et al. demonstrated advanced 4D imaging which is able to realize a 4 nm spectral resolution and near-diffraction-limit spatial resolution [57]. Significant advancements have been made in lensless imaging-based multispectral systems, offering compact and cost-effective solutions for spectral information capture.

4.3. Three-dimensional imaging

The conventional lens-based imaging process involves the mapping of 3D scene onto 2D images, which leads to the loss of depth information. However, 3D imaging technology has the capability to capture spatial 3D information, making it a promising tool in machine vision, and AR/VR. The integration of lensless computational imaging and 3D imaging presents numerous new opportunities. In 2017, Antipa et al. proposed the DiffuserCam, which requires pre-experimental calibration to obtain PSF patterns at different depths (Fig. 11c) [10]. Each PSF pattern can be considered as a linear system with spatial translation invariance. By combining this approach with a compressive sensing reconstruction algorithm based on sparse representation, the DiffuserCam enables spatial 3D imaging. Cai et al. extended this technique by implementing 4D light field imaging using the scattering media of DiffuserCam [118]. Metasurfaces can also be used as encoding elements. In 2019, Lin et al. designed a full-color polarization-dependent metalens array, which is able to capture light-field information and reconstruct the depth information of the scene [33]. In the same year, Guo et al. proposed a compact depth sensor based on metalens [119]. This system demonstrated the ability of depth estimation over a 10 cm range using a 3-mm-diameter metalens. These innovative approaches demonstrate the tremendous potential of lensless computational imaging, offering efficient solutions for capturing and reconstructing spatial 3D information.

4.4. Optical fiber imaging

Optical fibers are passive devices that can be bent at will to facilitate image transmission. Owing to their high flexibility and light weight, optical fibers have found wide use in medical and industrial applications. Lensless computational imaging has gained much popularity in optical fiber endoscopic imaging as it offers several advantages, such as compact design and precise reconstruction. In 2016, Porat et al. employed a speckle correlation method to achieve lensless fiber bundle imaging [120]. In 2020, Shekel et al. used fiber-bending-generated speckles to improve the working distance and background rejection in lensless micro-endoscopy [121]. In 2019, Shin et al. used a randomly encoded mask positioned at the end of a fiber optic bundle to build a lensless microendoscopic system with an end diameter of only a few hundred microns (Fig. 11d) [113]. In 2022, Wu et al. proposed an end-to-end lensless fiber imaging technique, which enables both high-resolution histological imaging and real-time tumor diagnosis [122]. This fiber-based diagnostic approach is compact and low-cost, making it clinically promising for single-use probes. It eliminates the need for cumbersome processes, making it both patient- and physician-friendly.

5. Conclusion and outlook

This review provides the principles and prospects of lensless camera, with emphasis on latest breakthroughs in optical modulation elements, image sensors, and reconstruction algorithms. Currently, traditional optical components pose notable constraints. Lensless camera offers a unique blend of encoding optics and decoding algorithms, providing imaging systems with design flexibility, cost-effectiveness, and the capacity to achieve high-dimensional data. This paradigm shift has unlocked significant advancements in various applications, including microscopic imaging, multispectral imaging, 3D imaging, and optical fiber imaging. These research findings paint a promising picture, wherein lensless computational imaging holds potential for applications in real-time medical diagnosis, portable device imaging, AR/VR devices, and other scenarios.

Despite the notable advantages, several challenges and limitations should be addressed to fully harness the potential of lensless computational imaging. A major obstacle lies in the limited capability of current optical modulation elements to efficiently encode high-dimensional information, leading to suboptimal reconstruction quality. It is imperative to develop metasurface-based optical modulation elements. This necessitates in-depth research into the encoding mechanisms of multi-dimensional light-field information, as well as the establishment of a comprehensive physical model of electromagnetic computation and diffraction light field. Furthermore, the efficacy of reconstruction algorithms strongly depends on accurate prior physical knowledge and data information, leading to limited generalization across diverse scenarios. To address this issue, it is essential to explore the application of plug-and-play optimization, algorithmic unfolding, and deep image prior techniques in solving inverse problems. By incorporating these methods alongside data prior, more accurate and reliable reconstructions can be achieved. Meanwhile, enhancing computational speed for real-

time image reconstruction and formulating reconstruction algorithms compatible with high-dimensional data are also future research goals. The demand for faster image reconstruction computational speed and higher photodetection image quality necessitates the development of large dynamic range, high spatial resolution photodetection, and high-performance computing chips. Developing integrated chips for photoelectric detection and reconstruction computation by incorporating mainstream algorithms is also crucial.

Currently, optical modulation elements based on metasurfaces, image reconstruction algorithms based on compressive sensing and deep learning, and high-performance detection and processing chips bring new development opportunities for lensless computational imaging. In order to realize the potential of lensless computational imaging, it is necessary to overcome the challenges related to encoding high-dimensional information, improve the accuracy of reconstruction algorithms, enhance computational speed, and develop advanced photodetection and computing chips. Researchers should evaluate application scenarios where lensless imaging surpasses traditional lens-based imaging and identify the distinctive characteristics that make lensless imaging a superior choice. These advancements pave the way for more efficient, high-quality, and practical lensless computational imaging systems.

Declaration of competing interest

The authors declare that they have no conflicts of interest in this work.

Acknowledgment

This work was supported by the National Natural Science Foundation of China (62235009).

References

[1] J. Wang, C. Wang, Optics in China, in: H. Selin (Ed.), Encyclopaedia of the History of Science, Technology, and Medicine in Non-Western Cultures, Springer Netherlands, Dordrecht, 2008, pp. 1790–1792.
[2] J. Al-Khalili, In retrospect: book of optics, Nature 518 (2015) 164–165, doi:10.1038/518164a.
[3] A.A. Khan, A.A. Laghari, S.A. Awan, Machine learning in computer vision: a review, EAI Endorsed Trans. Scalable Inf. Syst. 8 (2021) e4-e4, doi:10.4108/eai.21-4-2021.169418.
[4] R.J. Gove, CMOS image sensor technology advances for mobile devices, High Perform. Silicon Imaging (2020) 185–240.
[5] V. Goiffon, M. Estribeau, P. Magnan, Overview of ionizing radiation effects in image sensors fabricated in a deep-submicrometer CMOS imaging technology, IEEE Trans. Electron. Devices 56 (2009) 2594–2601, doi:10.1109/ted.2009.2030623.
[6] X. Wang, W. Wong, R. Hornsey, A high dynamic range CMOS image sensor with in-pixel light-to-frequency conversion, IEEE Trans. Electron. Devices 53 (2006) 2988–2992, doi:10.1109/ted.2006.885642.
[7] J.N. Mait, G.W. Euliss, R.A. Athale, Computational imaging, Adv. Opt. Photonics 10 (2018) 409–483, doi:10.1364/AOP.10.000409.
[8] V. Boominathan, J.K. Adams, J.T. Robinson, et al., PhlatCam: designed phase-mask based thin lensless camera, IEEE Trans. Pattern. Anal. Mach. Intell. 42 (2020) 1618–1629, doi:10.1109/TPAMI.2020.2987489.
[9] J.K. Adams, V. Boominathan, B.W. Avants, et al., Single-frame 3D fluorescence microscopy with ultraminiature lensless FlatScope, Sci. Adv. 3 (2017) e1701548 %J Science Advances, doi:10.1126/sciadv.1701548.
[10] N. Antipa, G. Kuo, R. Heckel, et al., DiffuserCam: lensless single-exposure 3D imaging, Optica 5 (2017) 1–9, doi:10.1364/optica.5.000001.
[11] Y. Zheng, Y. Hua, A.C. Sankaranarayanan, et al., A simple framework for 3D lensless imaging with programmable masks, in: 2021 IEEE/CVF International Conference on Computer Vision (ICCV), 2021, pp. 2583–2592, doi:10.1109/iccv48922.2021.00260.
[12] A.K. Singh, D.N. Naik, G. Pedrini, et al., Exploiting scattering media for exploring 3D objects, Light: Sci. Appl. 6 (2017) e16219-e16219, doi:10.1038/lsa.2016.219.
[13] K. Monakhova, K. Yanny, N. Aggarwal, et al., Spectral DiffuserCam: lensless snapshot hyperspectral imaging with a spectral filter array, Optica 7 (2020) 1298–1307, doi:10.1364/optica.397214.
[14] J. Wang, Y. Zhao, Lensless multispectral camera based on a coded aperture array, Sensors 21 (2021) 7757, doi:10.3390/s21227757.
[15] Y. Hua, S. Nakamura, M.S. Asif, et al., SweepCam — depth-aware lensless imaging using programmable masks, IEEE Trans. Pattern. Anal. Mach. Intell. 42 (2020) 1606–1617, doi:10.1109/TPAMI.2020.2986784.
[16] A. Greenbaum, W. Luo, B. Khademhosseinieh, et al., Increased space-bandwidth product in pixel super-resolved lensfree on-chip microscopy, Sci. Rep. 3 (2013) 1717, doi:10.1038/srep01717.
[17] Y. Gao, L. Cao, Motion-resolved, reference-free holographic imaging via spatiotemporally regularized inversion, Optica 11 (2024) 32–41, doi:10.1364/OPTICA.506572.
[18] Y. Gao, L. Cao, Iterative projection meets sparsity regularization: towards practical single-shot quantitative phase imaging with in-line holography, Light Adv. Manuf. 4 (2023) 37–53, doi:10.37188/lam.2023.006.
[19] A. Ozcan, E. McLeod, Lensless imaging and sensing, Annu. Rev. Biomed. Eng. 18 (2016) 77–102, doi:10.1146/annurev-bioeng-092515-010849.
[20] S. Jiang, P. Song, T. Wang, et al., Spatial- and Fourier-domain ptychography for high-throughput bio-imaging, Nat. Protoc. 18 (2023) 2051–2083, doi:10.1038/s41596-023-00829-4.
[21] Y. Fan, J. Li, L. Lu, et al., Smart computational light microscopes (SCLMs) of smart computational imaging laboratory (SCILab), Photonix 2 (2021) 19, doi:10.1186/s43074-021-00040-2.
[22] S. Jiang, C. Guo, T. Wang, et al., Blood-coated sensor for high-throughput ptychographic cytometry on a blu-ray disc, ACS Sens. 7 (2022) 1058–1067, doi:10.1021/acssensors.1c02704.
[23] S. Banerji, M. Meem, A. Majumder, et al., Imaging with flat optics: metalenses or diffractive lenses? Optica 6 (2019) 805–810, doi:10.1364/OPTICA.6.000805.
[24] Q. Zhang, Z. He, Z. Xie, et al., Diffractive optical elements 75 years on: from micro-optics to metasurfaces, Photonics Insights 2 (2023) R09, doi:10.3788/pi.2023.R09.
[25] T. Li, C. Chen, X. Xiao, et al., Revolutionary meta-imaging: from superlens to metalens, Photonics Insights 2 (2023) R01, doi:10.3788/pi.2023.R01.
[26] X. Xiao, Y. Zhao, X. Ye, et al., Large-scale achromatic flat lens by light frequency-domain coherence optimization, Light: Sci. Appl. 11 (2022) 323, doi:10.1038/s41377-022-01024-y.
[27] M.S. Asif, A. Ayremlou, A. Sankaranarayanan, et al., FlatCam: thin, lensless cameras using coded aperture and computation, IEEE Trans. Comput. ImAging 3 (2017) 384–397, doi:10.1109/tci.2016.2593662.
[28] B. Muminov, L.T. Vuong, Fourier optical preprocessing in lieu of deep learning, Optica 7 (2020) 1079–1088, doi:10.1364/OPTICA.397707.
[29] J. Wu, H. Zhang, W. Zhang, et al., Single-shot lensless imaging with Fresnel zone aperture and incoherent illumination, Light: Sci. Appl. 9 (2020) 53, doi:10.1038/s41377-020-0289-9.
[30] S.R. Gottesman, E.E. Fenimore, New family of binary arrays for coded aperture imaging, Appl. Opt. 28 (1989) 4344–4352, doi:10.1364/AO.28.004344.
[31] P.R. Gill, D.G. Stork, Lensless ultra-miniature imagers using odd-symmetry spiral phase gratings, Imaging Appl. Opt. (2013) Optica Publishing Group, Arlington, VirginiaCW4C.3, doi:10.1364/COSI.2013.CW4C.3.
[32] L. Zhang, H. Zhan, X. Liu, et al., A wide-field and high-resolution lensless compound eye microsystem for real-time target motion perception, Microsyst. Nanoeng. 8 (2022) 83, doi:10.1038/s41378-022-00388-w.
[33] R.J. Lin, V.-C. Su, S. Wang, et al., Achromatic metalens array for full-colour light-field imaging, Nat. Nanotechnol. 14 (2019) 227–231, doi:10.1038/s41565-018-0347-0.
[34] C. Jin, M. Afsharnia, R. Berlich, et al., Dielectric metasurfaces for distance measurements and three-dimensional imaging, Adv. Photonics 1 (2019) 036001, doi:10.1117/1.Ap.1.3.036001.
[35] E. Tseng, S. Colburn, J. Whitehead, et al., Neural nano-optics for high-quality thin lens imaging, Nat. Commun. 12 (2021) 6493, doi:10.1038/s41467-021-26443-0.
[36] Z. Shen, F. Zhao, C. Jin, et al., Monocular metasurface camera for passive single-shot 4D imaging, Nat. Commun. 14 (2023) 1035, doi:10.1038/s41467-023-36812-6.
[37] B. Leng, M. Chen, D. Tsai, Design, fabrication, and imaging of meta-devices, Acta Optica Sinica 43 (2023) 0822001.
[38] H.H. Barrett, F.A. Horrigan, Fresnel zone plate imaging of gamma rays; theory, Appl. Opt. 12 (11) (1973) 2686–2702, doi:10.1364/AO.12.002686.
[39] R.H. Dicke, Scatter-hole cameras for X-rays and gamma rays, Astrophys. J. 153 (1968) L101, doi:10.1086/180230.
[40] J.G. Ables, Fourier transform photography: a new method for X-ray astronomy, Publ. Astronom. Soc. Aust. 1 (1968) 172–173, doi:10.1017/S1323358000011292.
[41] G.L. Rogers, Gabor diffraction microscopy: the hologram as a generalized zone-plate, Nature 166 (1950) 237-237, doi:10.1038/166237a0.
[42] L.N. Mertz, N.O. Young, Fresnel transformation of images (Fresnel coding and decoding of images), optical instruments and techinques, in: Proceedings of the conference held in London, 1962.
[43] M.J.E. Golay, Point arrays having compact, nonredundant autocorrelations, J. Opt. Soc. Am. 61 (1971) 272–273, doi:10.1364/JOSA.61.000272.
[44] E.E. Fenimore, T.M. Cannon, Coded aperture imaging with uniformly redundant arrays, Appl. Opt. 17 (3) (1978) 337–347, doi:10.1364/AO.17.000337.
[45] F. Tian, J. Hu, W. Yang, GEOMScope: large field-of-view 3D lensless microscopy with low computational complexity, Laser. Photon. Rev. 15 (2021) 2100072, doi:10.1002/lpor.202100072.
[46] Y. Xue, I.G. Davison, D.A. Boas, et al., Single-shot 3D wide-field fluorescence imaging with a computational miniature mesoscope, Sci. Adv. 6 (2020) eabb7508, doi:10.1126/sciadv.abb7508.
[47] F. Tian, W. Yang, Learned lensless 3D camera, Opt. Express. 30 (2022) 34479–34496, doi:10.1364/OE.465933.

[48] Y.-H. Liu, T.-X. Qin, Y.-C. Wang, et al., Research advances in simple and compact optical imaging techniques, Acta Physica Sinica 72 (2023) 084205-084201-084205-084226, doi:10.7498/aps.72.20230092.
[49] M. Liu, W. Zhu, P. Huo, et al., Multifunctional metasurfaces enabled by simultaneous and independent control of phase and amplitude for orthogonal polarization states, Light: Sci. Appl. 10 (2021) 107, doi:10.1038/s41377-021-00552-3.
[50] Q. Jiang, L. Cao, L. Huang, et al., A complex-amplitude hologram using an ultrathin dielectric metasurface, Nanoscale 12 (2020) 24162–24168, doi:10.1039/d0nr06461k.
[51] N.A. Rubin, G. D'Aversa, P. Chevalier, et al., Matrix Fourier optics enables a compact full-Stokes polarization camera, Science 365 (2019) eaax1839, doi:10.1126/science.aax1839.
[52] J. Li, J. Liu, Z. Yue, et al., Polarization variable terahertz metasurface along the propagation path, Fundam. Res. (2023), doi:10.1016/j.fmre.2023.03.017.
[53] M. Wang, Y. Li, Y. Tang, et al., Nonlinear chiroptical holography with pancharatnam–berry phase controlled plasmonic metasurface, Laser. Photon. Rev. 16 (2022) 2200350, doi:10.1002/lpor.202200350.
[54] Y. Shen, X. Wang, Z. Xie, et al., Optical vortices 30 years on: OAM manipulation from topological charge to multiple singularities, Light: Sci. Appl. 8 (2019) 90, doi:10.1038/s41377-019-0194-2.
[55] N. Mao, J. Deng, X. Zhang, et al., Nonlinear diatomic metasurface for real and Fourier space image encoding, Nano Lett. 20 (2020) 7463–7468, doi:10.1021/acs.nanolett.0c02910.
[56] M. Khorasaninejad, Metalenses at visible wavelengths: diffraction-limited focusing and subwavelength resolution imaging, Science 352 (2016), doi:10.1126/science.aaf6644.
[57] X. Hua, Y. Wang, S. Wang, et al., Ultra-compact snapshot spectral light-field imaging, Nat. Commun. 13 (2022) 2732, doi:10.1038/s41467-022-30439-9.
[58] E. Arbabi, S.M. Kamali, A. Arbabi, et al., Full-Stokes imaging polarimetry using dielectric metasurfaces, ACS Photonics 5 (2018) 3132–3140, doi:10.1021/acsphotonics.8b00362.
[59] P. Huo, C. Zhang, W. Zhu, et al., Photonic spin-multiplexing metasurface for switchable spiral phase contrast imaging, Nano Lett. 20 (2020) 2791–2798, doi:10.1021/acs.nanolett.0c00471.
[60] N. Yu, Light propagation with phase discontinuities: generalized laws of reflection and refraction, Science 334 (2011) 333–337, doi:10.1126/science.1210713.
[61] S. Sun, Q. He, S. Xiao, et al., Gradient-index meta-surfaces as a bridge linking propagating waves and surface waves, Nat. Mater. 11 (2012) 426–431, doi:10.1038/nmat3292.
[62] X. Zhang, Z. Tian, W. Yue, et al., Broadband terahertz wave deflection based on C-shape complex metamaterials with phase discontinuities, Adv. Mater. 25 (2013) 4567–4572, doi:10.1002/adma.201204850.
[63] L. Liu, X. Zhang, M. Kenney, et al., Broadband metasurfaces with simultaneous control of phase and amplitude, Adv. Mater. 26 (2014) 5031–5036, doi:10.1002/adma.201401484.
[64] M. Khorasaninejad, Achromatic metalens over 60nm bandwidth in the visible and metalens with reverse chromatic dispersion, Nano Lett. 17 (2017) 1819–1824, doi:10.1021/acs.nanolett.6b05137.
[65] Z.-B. Fan, Z.-K. Shao, M.-Y. Xie, et al., Silicon nitride metalenses for close-to-one numerical aperture and wide-angle visible imaging, Phys. Rev. Appl. 10 (2018) 014005, doi:10.1103/PhysRevApplied.10.014005.
[66] S. Wang, P.C. Wu, V.C. Su, et al., Broadband achromatic optical metasurface devices, Nat. Commun. 8 (2017) 187, doi:10.1038/s41467-017-00166-7.
[67] M. Khorasaninejad, F. Capasso, Broadband multifunctional efficient meta-gratings based on dielectric waveguide phase shifters, Nano Lett. 15 (2015) 6709–6715, doi:10.1021/acs.nanolett.5b02524.
[68] S. Pancharatnam, Generalized theory of interference, and its applications, Proc. Indian Acad. Sci. - Sect. A 44 (1956) 247–262, doi:10.1007/bf03046050.
[69] M.V. Berry, Quantal phase factors accompanying adiabatic changes, Proc. R. Soc. Lond. A. Math. Phys. Sci. 392 (1984) 45–57, doi:10.1098/rspa.1984.0023.
[70] A. Dai, P. Fang, J. Gao, et al., Multifunctional metasurfaces enabled by multifold geometric phase interference, Nano Lett. 23 (2023) 5019–5026, doi:10.1021/acs.nanolett.3c00881.
[71] M.-K. Park, C.-S. Park, Y.S. Hwang, et al., Virtual-moving metalens array enabling light-field imaging with enhanced resolution, Adv. Opt. Mater. 8 (2020) 2000820, doi:10.1002/adom.202000820.
[72] X. Jing, R. Zhao, X. Li, et al., Single-shot 3D imaging with point cloud projection based on metadevice, Nat. Commun. 13 (2022) 7842, doi:10.1038/s41467-022-35483-z.
[73] V. Boominathan, J.K. Adams, M.S. Asif, et al., Lensless imaging: a computational renaissance, IEEE Signal. Process. Mag. 33 (2016) 23–35, doi:10.1109/MSP.2016.2581921.
[74] I. Daubechies, M. Defrise, C. De Mol, An iterative thresholding algorithm for linear inverse problems with a sparsity constraint, Commun. Pure Appl. Math. 57 (2004) 1413–1457, doi:10.1002/cpa.20042.
[75] J.M. Bioucas-Dias, M.A.T. Figueiredo, A new TwIST: two-step iterative shrinkage/thresholding algorithms for image restoration, IEEE Trans. Image Process. 16 (2007) 2992–3004, doi:10.1109/TIP.2007.909319.
[76] A. Beck, M. Teboulle, A fast iterative shrinkage-thresholding algorithm for linear inverse problems, SIAM J. Imaging Sci. 2 (2009) 183–202, doi:10.1137/080716542.
[77] S.P. Boyd, N. Parikh, E.K.-w. Chu, et al., Distributed optimization and statistical learning via the alternating direction method of multipliers, Found. Trends Mach. Learn. 3 (2011) 1–122, doi:10.1561/2200000016.
[78] W. Zhang, L. Cao, D.J. Brady, et al., Twin-image-free holography: a compressive sensing approach, Phys. Rev. Lett. 121 (2018) 093902, doi:10.1103/PhysRevLett.121.093902.
[79] F. Liu, J. Wu, L. Cao, Autofocusing of Fresnel zone aperture lensless imaging for QR code recognition, Opt. Express. 31 (2023) 15889–15903, doi:10.1364/OE.489157.
[80] H.C. Burger, C.J. Schuler, S. Harmeling, Image denoising: can plain neural networks compete with BM3D? in: 2012 IEEE Conference on Computer Vision and Pattern Recognition, 2012, pp. 2392–2399, doi:10.1109/CVPR.2012.6247952.
[81] C.J. Schuler, H.C. Burger, S. Harmeling, et al., A machine learning approach for non-blind image deconvolution, in: 2013 IEEE Conference on Computer Vision and Pattern Recognition, 2013, pp. 1067–1074, doi:10.1109/CVPR.2013.142.
[82] O. Ronneberger, P. Fischer, T. Brox, U-Net: convolutional networks for biomedical image segmentation, in: Medical Image Computing and Computer-Assisted Intervention–MICCAI 2015: 18th International Conference, 2015, pp. 234–241.
[83] Y. Wu, J. Wu, S. Jin, et al., Dense-U-net: dense encoder–decoder network for holographic imaging of 3D particle fields, Opt. Commun. 493 (2021) 126970, doi:10.1016/j.optcom.2021.126970.
[84] Y. Wang, H. Wang, M. Gu, High performance "non-local" generic face reconstruction model using the lightweight Speckle-Transformer (SpT) UNet, Opto-Electron. Adv. 6 (2023) 220049-220041-220049-220049, doi:10.29026/oea.2023.220049.
[85] A. Sinha, J. Lee, S. Li, et al., Lensless computational imaging through deep learning, Optica 4 (2017) 1117–1125, doi:10.1364/OPTICA.4.001117.
[86] K. Monakhova, J. Yurtsever, G. Kuo, et al., Learned reconstructions for practical mask-based lensless imaging, Opt. Express. 27 (2019) 28075–28090, doi:10.1364/OE.27.028075.
[87] S.S. Khan, V. Sundar, V. Boominathan, et al., FlatNet: towards photorealistic scene reconstruction from lensless measurements, IEEE Trans. Pattern. Anal. Mach. Intell. 44 (2022) 1934–1948, doi:10.1109/TPAMI.2020.3033882.
[88] M. Haris, G. Shakhnarovich, N. Ukita, Deep back-projection networks for super-resolution, in: 2018 IEEE/CVF Conference on Computer Vision and Pattern Recognition, 2018, pp. 1664–1673, doi:10.1109/CVPR.2018.00179.
[89] J. Wu, L. Cao, G. Barbastathis, DNN-FZA camera: a deep learning approach toward broadband FZA lensless imaging, Opt. Lett. 46 (2021) 130–133, doi:10.1364/OL.411228.
[90] H. Zhou, H. Feng, Z. Hu, et al., Lensless cameras using a mask based on almost perfect sequence through deep learning, Opt. Express. 28 (2020) 30248–30262, doi:10.1364/OE.400486.
[91] H. Zhou, H. Feng, W. Xu, et al., Deep denoiser prior based deep analytic network for lensless image restoration, Opt. Express. 29 (2021) 27237–27253, doi:10.1364/OE.432544.
[92] S.I. Nikolenko, Synthetic Data for Deep Learning, Springer Nature, Switzerland, 2021.
[93] E. Agustsson, R. Timofte, NTIRE 2017 challenge on single image super-resolution: dataset and study, in: 2017 IEEE Conference on Computer Vision and Pattern Recognition Workshops (CVPRW), 2017, pp. 1122–1131, doi:10.1109/CVPRW.2017.150.
[94] R. Horisaki, Y. Okamoto, J. Tanida, Deeply coded aperture for lensless imaging, Opt. Lett. 45 (2020) 3131–3134, doi:10.1364/OL.390810.
[95] Y. Peng, Q. Fu, F. Heide, et al., The diffractive achromat full spectrum computational imaging with diffractive optics, ACM Trans. Graph. 35 (2016) 1–11, doi:10.1145/2897824.2925941.
[96] F. Heide, Q. Fu, Y. Peng, et al., Encoded diffractive optics for full-spectrum computational imaging, Sci. Rep. 6 (2016) 33543, doi:10.1038/srep33543.
[97] S.-H. Baek, H. Ikoma, D.S. Jeon, et al., Single-shot hyperspectral-depth imaging with learned diffractive optics, in: 2021 IEEE/CVF International Conference on Computer Vision (ICCV), 2021, pp. 2631–2640, doi:10.1109/iccv48922.2021.00265.
[98] Y. Kitamura, H. Aikawa, K. Kakehi, et al., Suppression of crosstalk by using backside deep trench isolation for 1.12μm backside illuminated CMOS image sensor, 2012 International Electron Devices Meeting, 2012 24.22.21-24.22.24, doi:10.1109/IEDM.2012.6479093.
[99] A.Y.C. Chiou, C.C. Hsieh, An ULV PWM CMOS imager with adaptive-multiple-sampling linear response, HDR imaging, and energy harvesting, IEEE J. Solid-State Circuits 54 (2019) 298–306, doi:10.1109/JSSC.2018.2870559.
[100] W. Zhang, J. Suo, K. Dong, et al., Handheld snapshot multi-spectral camera at tens-of-megapixel resolution, Nat. Commun. 14 (2023) 5043, doi:10.1038/s41467-023-40739-3.
[101] L. Mennel, J. Symonowicz, S. Wachter, et al., Ultrafast machine vision with 2D material neural network image sensors, Nature 579 (2020) 62–66, doi:10.1038/s41586-020-2038-x.
[102] K.T. Tang, W.C. Wei, Z.W. Yeh, et al., Considerations of integrating computing-in-memory and processing-in-sensor into convolutional neural network accelerators for low-power edge devices, in: 2019 Symposium on VLSI Circuits, 2019, pp. T166–T167, doi:10.23919/VLSIC.2019.8778074.
[103] J. Park, S. Park, K. Cho, et al., 7.9 1/2.74-inch 32Mpixel-prototype CMOS image sensor with 0.64μm unit pixels separated by full-depth deep-trench isolation, in: 2021 IEEE International Solid- State Circuits Conference (ISSCC), 2021, pp. 122–124, doi:10.1109/ISSCC42613.2021.9365751.
[104] J.A. Leñero-Bardallo, R. Carmona-Galán, R.-V. Á, A wide linear dynamic range image sensor based on asynchronous self-reset and tagging of saturation events, IEEE J. Solid-State Circuits 52 (2017) 1605–1617, doi:10.1109/JSSC.2017.2679058.
[105] J. Zuo, J. Bai, S. Choi, et al., Chip-integrated metasurface full-Stokes polarimetric imaging sensor, Light: Sci. Appl. 12 (2023) 218, doi:10.1038/s41377-023-01260-w.
[106] F. Zhou, Y. Chai, Near-sensor and in-sensor computing, Nat. Electron. 3 (2020) 664–671, doi:10.1038/s41928-020-00501-9.
[107] D. Wang, S. Hao, B. Dkhil, et al., Ferroelectric materials for neuroinspired computing applications, Fundam. Res. (2023), doi:10.1016/j.fmre.2023.04.013.

[108] Z. Zhang, S. Wang, C. Liu, et al., All-in-one two-dimensional retinomorphic hardware device for motion detection and recognition, Nat. Nanotechnol. 17 (2022) 27–32, doi:10.1038/s41565-021-01003-1.
[109] J.H. Kim, C. Kim, K. Kim, et al., An ultra-low-power analog-digital hybrid CNN face recognition processor integrated with a CIS for always-on mobile devices, in: 2019 IEEE International Symposium on Circuits and Systems (ISCAS), 2019, pp. 1–5, doi:10.1109/ISCAS.2019.8702698.
[110] Z. Chen, H. Zhu, E. Ren, et al., Processing near sensor architecture in mixed-signal domain with CMOS image sensor of convolutional-kernel-readout method, IEEE Trans. Circuits Syst. I: Regular Pap. 67 (2020) 389–400, doi:10.1109/TCSI.2019.2937227.
[111] T.H. Hsu, Y.R. Chen, R.S. Liu, et al., A 0.5-V real-time computational CMOS image sensor with programmable kernel for feature extraction, IEEE J. Solid-State Circuits 56 (2021) 1588–1596, doi:10.1109/JSSC.2020.3034192.
[112] J. Tonnesen, V. Inavalli, U.V. Nagerl, Super-resolution imaging of the extracellular space in living brain tissue, Cell 172 (2018) 1108–1121 e1115, doi:10.1016/j.cell.2018.02.007.
[113] J. Shin, D.N. Tran, J.R. Stroud, et al., A minimally invasive lens-free computational microendoscope, Sci. Adv. 5 (2019) eaaw5595, doi:10.1126/sciadv.aaw5595.
[114] S. Seo, T.W. Su, D.K. Tseng, et al., Lensfree holographic imaging for on-chip cytometry and diagnostics, Lab Chip 9 (2009) 777–787, doi:10.1039/b813943a.
[115] G. Zheng, S.A. Lee, S. Yang, et al., Sub-pixel resolving optofluidic microscope for on-chip cell imaging, Lab Chip 10 (2010) 3125–3129, doi:10.1039/c0lc00213e.
[116] T. Nakamura, K. Kagawa, S. Torashima, et al., Super field-of-view lensless camera by coded image sensors, Sensors 19 (2019) 1329, doi:10.3390/s19061329.
[117] J. Chen, X. Ye, S. Gao, et al., Planar wide-angle-imaging camera enabled by metalens array, Optica 9 (2022) 431–437, doi:10.1364/optica.446063.
[118] Z. Cai, J. Chen, G. Pedrini, et al., Lensless light-field imaging through diffuser encoding, Light: Sci. Appl. 9 (2020) 143, doi:10.1038/s41377-020-00380-x.
[119] Q. Guo, Z. Shi, Y.W. Huang, et al., Compact single-shot metalens depth sensors inspired by eyes of jumping spiders, Proc. Natl. Acad. Sci. 116 (2019) 22959–22965, doi:10.1073/pnas.1912154116.
[120] A. Porat, E.R. Andresen, H. Rigneault, et al., Widefield lensless imaging through a fiber bundle via speckle correlations, Opt. Express. 15 (2016) 16835–16855 24, doi:10.1364/OE.24.016835.
[121] N. Shekel, O. Katz, Using fiber-bending-generated speckles for improved working distance and background rejection in lensless micro-endoscopy, Opt. Lett. 45 (2020) 4288–4291, doi:10.1364/OL.395839.
[122] J. Wu, T. Wang, O. Uckermann, et al., Learned end-to-end high-resolution lensless fiber imaging towards real-time cancer diagnosis, Sci. Rep. 12 (2022) 18846, doi:10.1038/s41598-022-23490-5.

Shuowen Li received her BS degree from the Cuiying Honors College, Lanzhou University in 2023. Then she became a PhD student of Optical Engineering at the Department of Precision Instruments, Tsinghua University. Her research interests are computational imaging and lensless imaging.

Liangcai Cao received his BS/MS and PhD degrees from Harbin Institute of Technology and Tsinghua University, in 1999/2001 and 2005, respectively. Then he became an assistant professor at the Department of Precision Instruments, Tsinghua University. He is now tenured professor and director of the Institute of Opto-electronic Engineering, Tsinghua University. He was a visiting scholar at UC Santa Cruz and MIT in 2009 and 2014, respectively. His research interests are holographic imaging and holographic display. He is a Fellow of the Optica and the SPIE.